Pharm Res (2014) 31:670–683
DOI 10.1007/s11095-013-1189-y

RESEARCH PAPER

Population PKPD Modeling of BACE1 Inhibitor-Induced Reduction in Aβ Levels *In Vivo* and Correlation to *In Vitro* Potency in Primary Cortical Neurons from Mouse and Guinea Pig

Juliette Janson • Susanna Eketjäll • Karin Tunblad • Fredrik Jeppsson • Stefan Von Berg • Camilla Niva • Ann-Cathrin Radesäter • Johanna Fälting • Sandra A. G. Visser

Received: 20 May 2013 / Accepted: 9 August 2013 / Published online: 3 October 2013

ABSTRACT

Purpose The aims were to quantify the *in vivo* time-course between the oral dose, the plasma and brain exposure and the inhibitory effect on Amyloid β (Aβ) in brain and cerebrospinal fluid, and to establish the correlation between *in vitro* and *in vivo* potency of novel β-secretase (BACE1) inhibitors.

Methods BACE1-mediated inhibition of Aβ was quantified in *in vivo* dose- and/or time-response studies and *in vitro* in SH-SY5Y cells, N2A cells, and primary cortical neurons (PCN). An indirect response model with inhibition on Aβ production rate was used to estimate unbound *in vivo* IC_{50} in a population pharmacokinetic-pharmacodynamic modeling approach.

Results Estimated *in vivo* inhibitory potencies varied between 1 and 1,000 nM. The turnover half-life of Aβ40 in brain was predicted to be 0.5 h in mouse and 1 h in guinea pig. An excellent correlation between PCN and *in vivo* potency was observed. Moreover, a strong correlation in potency was found between human SH-SY5Y cells and mouse PCN, being 4.5-fold larger in SH-SY5Y cells.

Conclusion The strong *in vivo-in vitro* correlation increased the confidence in using human cell lines for screening and optimization of BACE1 inhibitors. This can optimize the design and reduce the number of preclinical *in vivo* effect studies.

KEY WORDS Alzheimer's disease · amyloid β peptide · brain · cerebrospinal fluid · pharmacokinetic-pharmacodynamic modeling

ABBREVIATIONS

AD	Alzheimer's disease
APP	Amyloid precursor protein
Aβ	Amyloid β peptide
BACE1	β-site APP-cleaving enzyme 1
CSF	Cerebrospinal fluid
CV	Coefficient of variation
PCN	Primary cortical neurons
sAPPβ	Soluble N terminal fragment of APP

INTRODUCTION

Alzheimer's disease (AD) is a devastating progressive disease with gradual cognitive decline including memory loss, personality changes, and difficulties in performing routine tasks (1–3). The pathological hallmarks of AD are extracellular amyloid plaques and intracellular neurofibrillary tangles, neurodegeneration and brain atrophy. A growing body of pathological,

Electronic supplementary material The online version of this article (doi:10.1007/s11095-013-1189-y) contains supplementary material, which is available to authorized users.

J. Janson (✉) • K. Tunblad
Modeling & Simulation, DMPK, Innovative Medicines CNSP AstraZeneca SE-15185, Södertälje, Sweden
e-mail: juliettejanson@yahoo.com

S. Eketjäll • F. Jeppsson • C. Niva • A.-C. Radesäter
Neuroscience, Innovative Medicines CNSP AstraZeneca SE-15185, Södertälje, Sweden

S. Von Berg
Medical Chemistry, Innovative Medicines CNSP AstraZeneca SE-15185, Södertälje, Sweden

J. Fälting
Project Management, Innovative Medicines CNSP AstraZeneca SE-15185, Södertälje, Sweden

S. A. G. Visser
Global DMPK Centre of Excellence, Innovative Medicines CNSP AstraZeneca, SE-15185, Södertälje, Sweden

biomarker, genetic, and mechanistic data suggests that amyloid β (Aβ) amyloidosis, and the subsequent deposition of Aβ in plaques, play a key role in the pathogenesis of AD (4–7). Strong genetic evidence has been reported for a connection between the amyloid precursor protein (APP), Aβ and AD. People with a duplication of the APP gene or a mutation in presenilin, a component of the γ-secretase enzyme complex, develop AD 10–15 years earlier than non-carriers (5,7,8).

Aβ variants, such as Aβ40 and Aβ42, are produced by sequential cleavage of the APP by β- and γ-secretase, with Aβ42 appearing most pathogenic (9–12). β- or γ-secretase inhibitors and γ-secretase modulators can lower central Aβ40 and Aβ42 levels. For this reason, these are pursued as potential disease-modifying treatments for AD (13). To date, γ-secretase inhibition has been the most studied mechanism for reducing Aβ in clinical trials. However, so far no therapeutic success, in the form of slowing cognitive decline, has been demonstrated (6,13–15). The underlying reason for failure could have been the marginal lowering of central Aβ in these trials (16). The validity of the amyloid-lowering hypothesis can only be tested with drugs that substantially lower Aβ over the dosing interval (16).

The β-secretase enzyme is a promising target for reducing brain Aβ. Two homologues of the transmembrane aspartic protease β-secretase are known: BACE1 and BACE2 (17–21). BACE1 has been suggested to be the rate-limiting step in the production of Aβ (22). BACE1 protein levels and activity are up-regulated in brains of patients with sporadic AD (23). Moreover, APP that carries the Swedish mutation has a higher affinity for BACE1, with an increased Aβ formation and early onset of AD (19,24). In contrast, an APP mutation (APPA673T) with reduced affinity to BACE1 seems to protect against AD (25). In addition, BACE1 is required for the development of age-associated plaque pathology (26).

Drug-induced BACE1 inhibition, with a reduction in sAPPβ and/or Aβ40/42, has been reported in wild-type mice (27–30), transgenic mice (30–36), rats (37–39), guinea pigs (29,40), and non-human primates (29,41). Plasma, brain, and cerebrospinal fluid (CSF) Aβ levels have been reported in these species which allowed for exploration of the relationship between these three compartments. Reduced sAPPβ and Aβ in plasma and CSF have been demonstrated in human through BACE1 inhibition which was correlated to observations in preclinical species (42). Taken together, Aβ40, Aβ42, and sAPPβ are well-documented biomarkers for target engagement of BACE1 inhibitors, both in animals and in humans.

A quantitative understanding of *in vivo* target engagement and the animal-human correlation are essential to the confident selection of a new chemical entity that could reduce human Aβ levels enough to test the amyloid hypothesis (16). BACE1 inhibitors can be screened *in vitro* with a relatively simple biochemistry assay, consisting of a solution with substrate and enzyme (43). In cells, BACE1 inhibition can be monitored by reducing secretion of sAPPβ by wild-type SH-SY5Y, and Aβ40 by N2A cells into the medium (29,43). Moreover, inhibition of Aβ secretion can also be studied in cultures of primary cortical neurons (16). Differences regarding potency may occur between the different *in vitro* assays, not only due to sequence and expression variations in target and substrate, but also due to differences in the compounds' ability to reach the target.

The first aim of this investigation was to quantify the *in vivo* time-course between exposure and Aβ effect of oral dosing by novel BACE1 inhibitors in mouse and guinea pig. A population pharmacokinetic-pharmacodynamic (PKPD) approach was used for a simultaneous analysis of all *in vivo* time-course data of multiple compounds. This allowed for quantification of system-specific parameters (turnover-rate of Aβ and I_{max}), separately from compound-specific parameters (PK and potency). The second aim was to assess the correlation between *in vitro* and *in vivo* potency. The *in vivo* IC_{50} was correlated to the *in vitro* potency from primary cortical neurons. In a third step, the correlation of potency in various *in vitro* assays was investigated. The findings in this paper support the understanding of the translatability between *in vitro* assays and *in vivo* models, and between different species. This conceptual approach aims to support optimization of the screening cascade for novel BACE1 inhibitors *via* a change in the design and a reduced number of *in vivo* studies.

MATERIALS AND METHODS

Drugs and Chemicals

The BACE1 inhibitors were synthesized internally at the Department of Medicinal Chemistry, AstraZeneca in Södertälje, Sweden. All chemicals were purchased from Sigma-Aldrich (Saint Louis, MO, USA). A number of the new chemical entities reported in this paper have recently been published in the scientific or patent literature and are referred to in Table I (28,29,40).

Animals and Animal Handling

Rodent experiments were performed in accordance with relevant guidelines and regulations provided by the Swedish Board of Agriculture. The ethical permissions were provided by an ethical board specialized in animal experimentations (Stockholm North Animal Research ethical Board). All compounds were administered per oral in solutions with the fast majority consisting of 5% dimethylacetamide (DMA) and 20% hydroxypropyl-β-cyclodextrin (HPβCD) in 0.3 M Gluconic acid (pH 3).

Table I Population Parameter Estimates for *in vivo* IC_{50} in Mouse Based on Unbound Brain Concentrations, and *In Vitro IC50* in Primary Cortical Neurons, SH-SY5Y Cells and N2A Cells (± standard deviation), as well as Plasma Protein (PPB) and Brain Tissue Binding. *In Vivo* IC_{50} Estimates are Presented with Relative Error of the Mean (REM). TR = Time/dose Response Data, DR = Dose Response Data Available Only

Compound	Experimental design	IC_{50} *in vivo* (nM)	IC_{50} mouse primary neurons (nM)	IC_{50} SH-SY5Y cell line (nM)	IC_{50} N2A cells (nM)	Mouse PPB (% free)	Brain Tissue Binding (% free)
1[a]	TR	76 (17%)	28 ± 13	24 ± 11	39	12	8.3
2[b]	TR	247 (12%)	51 ± 16	17 ± 4	32	2.7	7.9
3[c]	TR	3.9 (10%)	2.7 ± 0.8	0.2 ± 0.2	0.6	1.5	1.0
4[d]	TR	99 (11%)	53 ± 57	8.6 ± 4.3	49	11	4.6
5	TR	72 (13%)	34 ± 18	12 ± 4	23	9.8	3.7
6[e]	TR	121 (11%)	64 ± 38	8.3 ± 2.6	82	8.9	8.8
7	DR	261 (9.1%)	360 ± 139	29 ± 10		4.1	2.7
8[f]	TR	173 (10%)	204 ± 21	22 ± 5		4.4	2.6
9	DR	3.9 (32%)	4.0 ± 0.1	2.2 ± 0.3		0.6	0.53
10	DR	64 (14%)	71 ± 10	11 ± 4		3.1	1.1
11	DR	159 (11%)	302 ± 138	33 ± 13		7.1	2.2
12	DR	12 (24%)	10 ± 2	< 1		10	6.8
13	DR	189 (22%)	98 ± 31	12 ± 10		2.3	1.6
14	DR	1130 (15%)	904 ± 587	121 ± 112		8.4	19
15[g]	DR	64 (24%)	30 ± 4	11 ± 2		52	16
16[h]	DR	6.7 (23%)	40 ± 6	2.9 ± 0.3		9.6	1.1
17[i]	DR	470 (16%)	183 ± 107	49 ± 26		16	9.8
18	DR	227 (16%)	140 ± 23	13 ± 17		5.4	1.7
19	DR	56 (15%)	10 ± 11	5.1 ± 0.2		6.1	1.7
20	DR	99 (19%)	70 ± 5	8.0 ± 5.1		4.5	1.5
21	DR	474 (23%)	36 ± 2	24 ± 3		19	9.5
22	DR	111 (52%)	22 ± 5	4.9 ± 1.5		5.8	1.7
23	DR	92 (18%)	163 ± 12	26 ± 0.4	88	4.1	1.6
24	DR	962 (16%)	245 ± 238	81 ± 20		15	12
25[j]	DR	244 (13%)	127 ± 4	59 ± 29	138	4.2	2.0
26	DR	375 (15%)	120 ± 84	124 ± 1		11	6.0
27	DR	240 (15%)	110 ± 78	39 ± 6		2.9	5.1
28	TR	508 (14%)	299 ± 93	46 ± 7		31	10
29	TR	226 (13%)	129 ± 13	48 ± 3		14	3.9
30[k]	TR	11 (7.7%)	3.4 ± 5.3	0.8 ± 0.3	1.8	1.8	0.6
31	DR	169 (27%)	258 ± 22	34 ± 7		5.9	2.7
32	TR	28 (10%)	31 ± 6	2.7 ± 0.5	9.3	6.4	1.9

Compounds published elsewhere with 1: compounds as published in (40); 2: compound code as published in (28) and 3 as published in (29); [a] 1; [b] 2:S-32, 3; [c] 2:R-41; [d] 2:S-16; [e] 2:S-25; [f] 2:S-10; [g] 2:37; [h] 2:35; [i] 1; [j] 2:R-20; [k] 1: R-19

Mouse *In Vivo* Experiments

Female C57BL/6 mice (Harlan Laboratories, The Netherlands) were randomized into different cages upon arrival. They were kept in conventional housing and were fed standard rodent chow and tap water *ad libitum*. The mice were acclimatized over a period of at least 7 days prior to study start. Before administration of the drug mice were weighed to calculate the dose volume, after which the vehicle or compound solution was administered as a single dose by oral gavage. Eleven compounds were run in a time-response design and 21 compounds in a dose–response design. One dose at a single time point typically included 6 compound treated animals and time-matched with 6 vehicle treated mice. A study consisted of a maximum of 36 mice per study. Blood was withdrawn from mice by heart puncture under isoflurane anesthesia into pre-chilled microtainer tubes containing EDTA. Blood samples were immediately put on ice prior to centrifugation. Plasma was prepared by centrifugation for 10 min (3,000 × *g* at 4°C) within 20 min from sampling. The

recovered plasma was collected and frozen. After blood sampling, mice were sacrificed by decapitation followed by brain samples collection. Cerebellum and olfactory bulbs were removed and forebrain was divided into left and right hemispheres. The hemispheres were weighed and snap-frozen.

Guinea Pig *In Vivo* Experiments

Male albino Dunkin-Hartley guinea pigs (HB Lidköpings Kaninfarm, Sweden) were randomized into different cages on arrival. They were kept in conventional housing and were fed standard guinea pig chow and tap water *ad libitum*. The guinea pigs were acclimatized over a period of at least 7 days prior to study start. Before administration of drug or vehicle the guinea pigs were weighed to calculate administration volume and a single dose was orally administered. Typically, a dose- and time-point included 8 compound-treated animals, matched with 8 vehicle-treated animals. Three compounds were run in a time-response design and one compound in a dose–response design. CSF sampling was performed from the cisterna magna by puncturing the atlanto-occipital membrane using a small cannula under isoflurane anesthesia. The sample was then centrifuged for 1 min at approximately 3,000×*g* at 4°C. The CSF supernatant was collected and snap-frozen. Immediately after the CSF sampling, blood was collected by heart puncture into pre-chilled microtainer tubes containing EDTA. Blood samples were immediately put on ice prior to centrifugation. Plasma was prepared by centrifugation for 10 min at approximately 3,000*g* at 4°C within 20 min from sampling. The recovered plasma was collected and immediately frozen. After blood sampling, the animals were sacrificed by decapitation and brains were dissected. Cerebellum and olfactory bulbs were removed and cerebrum was divided into left and right hemispheres. Immediately after isolation, hemispheres were weighed and snap-frozen.

Aβ Measurement of *In Vivo* Plasma, CSF and Brain Samples

Brain tissues were homogenized/sonicated in 1:18 (w/v) (1:20 for guinea pig) 0.2% diethylamine (DEA) with 50 mM NaCl, followed by ultracentrifugation. Recovered supernatants (soluble Aβ) were neutralized to pH 8.0 with 2 M Tris–HCl. For the mouse samples, Aβ40 levels in DEA brain extracts and Aβ40 levels in plasma were analyzed using a commercial Aβ1-40 Enzyme-Linked-Immuno-Sorbent Assay (ELISA) kit (#KMB3481, Invitrogen, Camarillo, CA). For the guinea pig samples, Aβ40 and Aβ42 levels in DEA brain extracts, CSF and plasma were analyzed using commercial Aβ1-40 (#KHB3482, Invitrogen, Camarillo, CA) and Aβ1-42 (#80177 RUO, Innogenetics, Gent, Belgium) ELISA kits. The lower limit of quantification (LLOQ) was determined for each immunoassay plate based on the lowest standard point with CV <20% and an accuracy (back-calculated concentrations) of 80–120%.

Plasma and Brain Exposure Analysis

Plasma samples and standards were precipitated with acetonitrile containing internal standard. After centrifugation, supernatant was transferred to a new 96-well plate, diluted with mobile phase, and injected on the LC/MS/MS system (43). Frozen mouse brains were weighed and ice-cold Ringer solution (2 volumes per weight) was added. Brains were sonicated using a Multi-element probe SONICS VCX 500 (Newtown, CT, USA). To 50 µL homogenized tissue 150 µL ice-cold acetonitrile containing an internal standard was added in a precipitation plate (96-well PP-plate, Waters, Milford, MA, USA). After mixing and centrifugation (4°C, 4,000 rpm, 20 min), supernatant was transferred to an analysis plate (PP-plate, Waters) and analyzed by LC/MS/MS (44). Since brains were not perfused prior to exposure analysis, a volume of 1.3% of blood in brain and the concentration of compound in plasma were used to calculate the brain concentration (45,46). The free concentration of compound in plasma and brain was calculated using the plasma protein and brain tissue binding data, respectively (see below).

Brain Tissue Binding

The fraction of unbound concentrations in brain was determined in a rat brain slice uptake method (47,48). In short, male Sprague–Dawley rats were decapitated under isoflurane anesthesia. The brain was immersed in ice-cold oxygenated extracellular fluid (ECF) buffer. Coronal slices (300 µm) of the striatal area were pre-incubated in 10 mL ECF buffer for 5 min at 37°C followed by incubation with 1 µM compound in ECF buffer (5 h at 37°C under 5% CO_2 in oxygen). After incubation, the brain slices were weighed and homogenized in 9 volumes (w/v) of ECF buffer with a sonicator. The slice homogenates and ECF buffer were stored at −20°C prior to analysis. To 50 µL homogenised tissue 150 µL ice-cold acetonitrile containing an internal standard was added in a precipitation plate. After mixing and centrifugation (4°C, 4,000 rpm, 20 min), the supernatant was transferred to the analysis plate and analyzed by LC/MS/MS.

Plasma Protein Binding

Equilibrium dialysis with an in-house equilibrium dialysis plate was used to determine the fraction unbound in female C57BL/6 mouse and male Dunkin-Hartley guinea pig plasma. Dialysis of 10 µmol/L compound in plasma was performed against phosphate buffered saline. A reference plasma sample with compound was stored in the freezer overnight. After incubation for 18 h at 37°C on a shaking

table, aliquots of the plasma and buffer samples were transferred from the dialysis plate to Waters deep 96-cell plates with glass inserts. All samples were precipitated with three volumes of ice-cold acetonitrile containing internal standard, followed by 10 min of shaking. Samples were centrifuged at 4,000 rpm, 4°C for 20 min, and supernatants were analyzed by LC-MS/MS.

SH-SY5Y Cell Assay

SH-SY5Y cells (human neuroblastoma cell line) were obtained from ATCC (Manassas, VA, USA) and cultured in DMEM/F-12 with Glutamax, 10% fetal calf serum and 1% non-essential amino acids. The test compound was incubated with cells for 16 h at 37°C, 5% CO_2 at a final concentration of 1% DMSO. Meso Scale Discovery (MSD; Gaithersburg, MD, USA) plates were used for the detection of sAPPβ release. MSD sAPPβ plates were blocked in 3% BSA in Tris wash buffer for 1 h at room temperature (RT) and washed in Tris buffer. 20 µL medium was transferred to the 384-well microplate, incubated at RT for 2 h followed by washing with Tris buffer. 10 µL detection antibody was added (1 nM) followed by incubation at RT for 2 h followed by washing with Tris buffer. 40 µL Read Buffer was added and the plates were read in a SECTOR Imager 6000 (MSD). In addition, the cells incubated with test compound were analyzed for any cytotoxic effects of the compounds using the ViaLightTM Plus cell proliferation/cytotoxicity kit (Cambrex BioScience Rockland, Maine, USA) according to the manufacturer's instructions. Reported values were means of $n \geq 2$ determinations, standard deviation ≤10%.

Neuro-2a Cells

Mouse Neuro-2a (N2A) cells were grown in medium (10% Foetal Bovine Serum (Sigma-Aldrich), 1% 10 mM Hepes, 1% MEM-NEAA and 88% MEM with Glutamax (all InVitrogen, Camarillo, CA, USA), seeded at a density of 40,000 cells/100 µL/well into 96-well tissue culture treated plates (Costar, Corning, Tewksbury, MA, USA) and incubated for 24 h at 37°C and 5% CO_2. At the following day the medium was changed to 100 µl medium containing compounds with a final concentration of 1% DMSO and plates were incubated for 18 h at 37°C and 5% CO_2. The amount of released Aβ into the culture medium was measured using a solid phase sandwich ELISA from MSD. Briefly, cell medium was transferred to MSD triplex plates with Aβ38, Aβ40 and Aβ42 capture antibodies. Primary sulfo-tagged detection antibody specific for the N-terminus of Aβ (4G8) was added and the plate was incubated over night at 4°C. The plate was processed according to the manufacturer's instructions and read on a Sector Imager 6000 (MSD). Aβ40 concentration in medium was analyzed using a Biosource ELISA kit KMB3481 (Invitrogen) at RT. Samples were incubated for 2 h followed by a wash. Thereafter, each well was incubated with 100 µL anti-Aβ40 for 1 h followed by washing. Subsequently, 100 µL of ant-rabbit IgG-HRP was added and incubated for 30 min followed by washing. This was followed by the addition of 100 µl stabilized chromogen to each well. The strips were incubated for up to 30 min in the dark, followed by the addition of 100 µL stop solution to each well, and were then read within 2 h in a SpectraMax (Molecular Devices, Sunnyvale, CA, USA) at 450 nm.

Mouse and Guinea Pig Primary Cortical Neurons

Primary cortical cells from foetal C57BL/6 mice at embryonic day 16 or from foetal Dunkin-Hartley guinea pigs embryonic 25–27 day were isolated. The cortices were collected in warm calcium and magnesium free Earle's Balanced Salt Solution (CMF-EBSS) containing 0.25% trypsin and 2 U/ml DNAse. After 1 h at +37°C and 5% CO_2, the trypsin/DNAse solution was removed and the cortices were washed 3 times in warm CMF-EBSS. Fresh CMF-EBSS was added to 10-15 ml and the cortices were gently triturated with flame polished pipettes to separate the cells. The cell solution was transferred to a 50 ml Falcon tub containing medium (10% HamsF12; 10% Foetal Bovine Serum; 1% 10 mM Hepes; 1% 2 mM L-Glutamine; 0.5% 50 U/0.5 mg Penicillin-Streptomycin and 77.5% DMEM w/4.5 g/L-Glucose), and filtered through a Cell Strainer 100 µm (BD Falcon, Fisher Scientific, Göteborg, Sweden) to remove clumps. Cells were plated onto 96-well poly-D-lysine coated plates at a density of 200,000 cells/200 µl/well. After 5 days in culture, the medium was exchanged to 50 µl (for Aβ42 measurements) or 100 µl (for Aβ40 measurements) medium containing compounds with a final concentration of 1% DMSO, incubated for 16 h at 37°C and 5% CO_2. The amount of released Aβ in culture medium was measured using a solid phase sandwich ELISA for cells from C57BL/6 mice (mouse βAmyloid 1–40, KMB3481, Invitrogen) and for guinea pig neurons (human βAmyloid 1–40, INNOTEST 80177, Innogenetics, Gent, Belgium) according to manufacturer's instructions. The absorbance of each well was read at 450 nm (SpectraMax) within 2 h after adding stop solution. The cytotoxic effect of compounds was directly evaluated on the cell plates utilizing a commercial cell proliferation/cytotoxicity kit based on luciferase reaction on ATP released by lyzed cells.

Pharmacokinetic-Pharmacodynamic Analysis

Aβ levels in brain and plasma were normalized to control levels and expressed as percentage change of the mean Aβ levels in the vehicle group, obtained from animals sacrificed at the same time point after dose in the same experiment. A total of 32 compounds in mice and 4 compounds in guinea pig were

tested in single dose, dose- and/or time-response (DR and/or TR) studies (Tables I and II, and Supplementary Material 1). In total, data from 829 mice and 186 guinea pigs on active treatment were included in the population analysis to assess the PKPD properties of the compounds. For the compounds tested in a time-response design, the relationship between brain exposure and plasma exposure was explored. A linear correlation was observed for these compounds. This relationship could not be explored for the compounds studied in a dose–response design. Therefore, the observed free brain or plasma concentration values were used as drivers for the effect in the modeling procedures. In this way, it was avoided to make any assumptions on the PK profile and brain distribution.

Simultaneous population modeling of all *in vivo* data per species was performed using an indirect response model with inhibition on the production rate (49) to estimate the unbound brain concentration giving 50% inhibition (IC_{50}) and turnover rate of Aβ.

$$\frac{d(A\beta)}{dt} = k_{in} \cdot Drug - k_{out} \tag{1}$$

$$Drug = \left(1 - \frac{I_{\max} \cdot C^n}{IC_{50}^n + C^n}\right) \tag{2}$$

where k_{in} and k_{out} represent production and turnover of Aβ, respectively, I_{max} was the maximum drug-induced Aβ inhibition, C was the compound concentration and n was the sigmoidicity factor. k_{out} and I_{max} were estimated jointly for all compounds as system-specific parameters. In contrast, the IC_{50} was estimated as a compound-specific parameter. Not for all compounds sufficient pharmacokinetic information was available; therefore the observed concentration of the compound in brain was used to estimate its IC_{50} on brain Aβ levels. In the PKPD analysis of CSF Aβ levels, the observed unbound concentration of the compound in plasma was used. To avoid I_{max} estimates to become larger than 1, it was defined following Eq. 3 in the guinea pig analysis of brain Aβ40.

$$I_{\max} = \left(\frac{e^{Theta(1)}}{1 + e^{Theta(1)}}\right) \tag{3}$$

Proportional and/or additive error models were investigated and selected based on minimum value of the objective function (MVOF). All population modeling was performed by a population approach using NONMEM software (Version 7.1.0, ICON Development Solutions, Hanover, MD).

In the *in vitro* data analysis, individual Aβ or sAPPβ observations were used and the test concentration was directly linked to the response using Eq. 2. For the visual representation of compound 5 and 1 (Figs. 1 and 2) PK and PKPD graphs, the PK parameters (absorption rate constant, clearance and volume) were estimated from the plasma or brain concentration data using WinNonlin (Version 5.2, Pharsight Co., Mountain View, CA, USA) using a 1-compartment model. Simulations, using the estimated PK parameters and the appropriate population modeling outcome, were carried out using Berkeley Madonna (Version 8.3.11, University of California, Berkeley, CA, USA). Prediction intervals were calculated using 1,000 runs in the Euler's method in Berkeley Madonna entering compound exposure and population effect and error estimates into the model. *In vitro-in vivo* correlations were evaluated using the Pearson's correlation coefficient.

RESULTS

Modeling of Brain Aβ40 in Mouse

All *in vivo* tested BACE1 inhibitors exhibited concentration- and time-dependent lowering of plasma and brain Aβ40 levels. Compound 5 is shown in Fig. 1 as an example in mice. After an oral dose of 50, 75, 100 or 300 μmol/kg, the plasma exposure increased more than linear with increased dose (Fig. 1a). The PK profiles were fit simultaneously. The best fit was obtained with a one-compartment model with an absorption rate constant of 0.89 h^{-1} (CV 6.5%), apparent clearance 12.6 L/h/kg (CV 12%) and apparent volume 5.5 L/kg (CV 39%) allowing for a dose-dependent relative bioavailability with 2.7-fold increase in exposure when the dose was doubled. While the maximum concentration in

Table II Population Parameter Estimates for *In Vivo* IC_{50} in Guinea Pig Based on Unbound Brain Concentrations, and *In Vitro* IC_{50} in Primary Cortical Neurons and SH-SY5Y Cells as well as Plasma Protein (PPB) and Brain Tissue Binding. *In Vivo* IC_{50} Estimates are Presented with Relative Error of the Mean (REM). TR = Time/Dose Response Data, DR = Dose Response Data Available Only

Compound	Experimental design	IC_{50} guinea pig *in vivo* (nM)	IC_{50} guinea pig primary neurons (nM)	IC_{50} SH-SY5Y cell line (nM)	Guinea pig PPB (% free)	Brain Tissue Binding (% free)
1	TR	59 (25%)	12 ± 11	24 ± 11	18	8.3
2	TR	107 (7.0%)	25 ± 13	17 ± 4	16	7.9
3	TR	0.92 (12%)	2.0 ± 1.3	0.2 ± 0.2	0.87	1.0
4	DR	51 (17%)	22 ± 14	8.6 ± 4.3	19	4.6

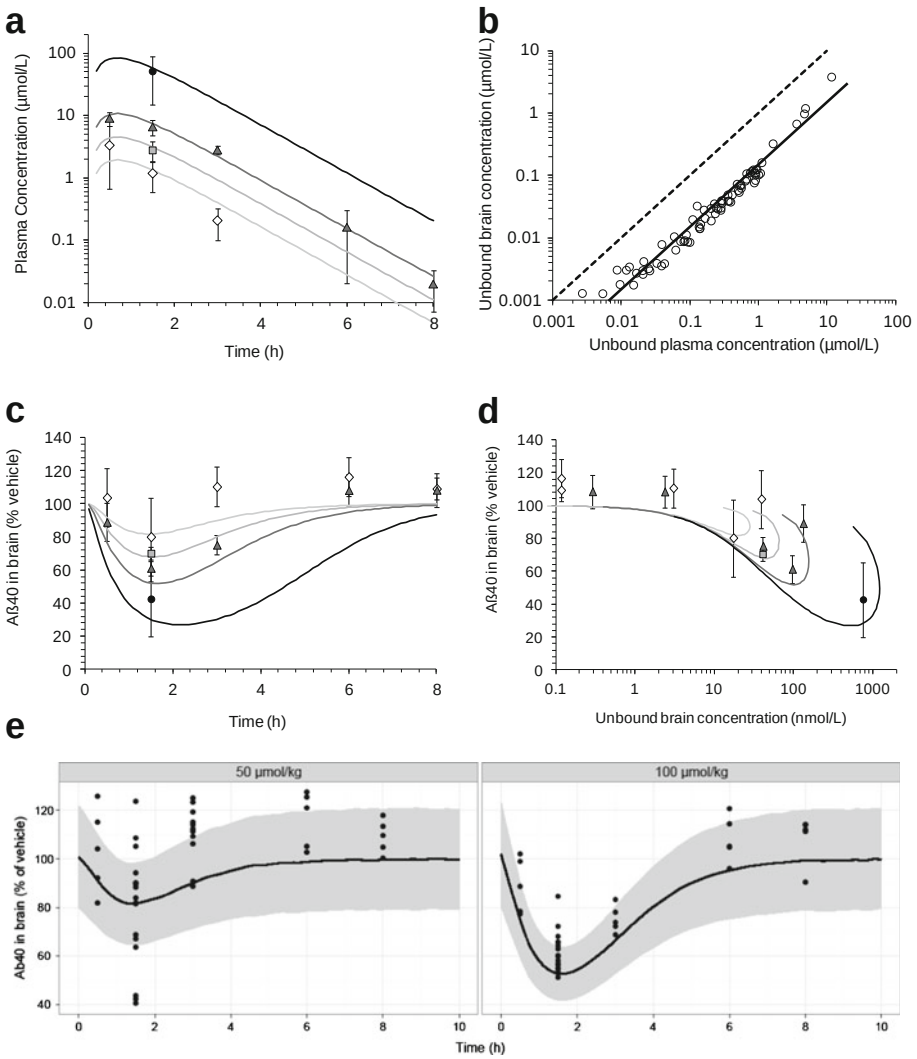

Fig. 1 Compound 5 dosed at 50 (diamonds), 75 (squares), 100 (triangles) or 300 (circles) μmol/kg p.o. to female C57BL/6 mice at $t = 0$. (**a**) Mean ± SD observed and fitted by naïve pooled analysis in WinNonlin plasma exposure. (**b**) Unbound plasma *versus* unbound brain exposure. (**c**) Mean ± SD observed and population fitted Aβ40 (% change from vehicle) in brain after oral dosing. (**d**) Mean ± SD observed and population fitted unbound brain concentrations *versus* Aβ40 inhibition in brain. (**e**) Individual time *versus* Aβ40 in brain observations and the 95% prediction interval after a 50 and 100 μmol/kg dose.

plasma was observed at 30 min after dose, the model-predicted maximum concentration was at 40 min after dose. The ratio between unbound plasma and brain concentration relationship was 0.15 and linear for all time-points and doses (Fig. 1b).

While the maximum plasma concentration was observed at 0.5 h after the dose, maximum effect on Aβ40 in brain (relative to vehicle levels) was observed at 1.5 h, indicating a delay in effect (Fig. 1c). This delay in effect was clearly visible by the appearance of a hysteresis loop in the brain Aβ40 *versus* unbound brain concentration (Fig. 1d). Population *in vivo* potency parameter estimates in mice are listed in Table I, and the population estimates for the system-specific parameters are listed in Table III. The value of k_{out} for brain Aβ40 was estimated at 1.5 h^{-1}, which corresponds to a turnover half-life of 28 min. The maximum inhibition of Aβ40 was estimated at 85%. The inclusion of a slope factor n did not improve the estimates and was therefore fixed to 1. To evaluate the goodness-of-fit, the variability on the population estimates was used to explore the 95% prediction interval, by simulation of 1,000 runs at doses 50 and 100 µmol/kg and calculation of its mean and interval using the PK and PD parameter estimates. The results are shown in Fig. 1e.

Goodness-of-fit plots are shown in Fig. 3a and b. A clear correlation between observed and predicted was present ($R = 0.73$, $P < 0.01$). The goodness-of-fit was also evaluated by plotting the conditional weighted residuals (CWRES) *versus* time. The CWRES were balanced around 0 with a deviation at 6 and 24 h (Fig. 3b), but in both cases 0 was included in the 95% confidence interval (CI, 6 h–0.5–2.8 and 24 h–0.2–1.7). 4.7% of observations had a CWRES outside the ±1.96 window.

Modeling of Brain and CSF Aβ40 in Guinea Pig

Four compounds were evaluated *in vivo* in male Dunkin Harley guinea pig. Three compounds included both time- and dose–response data, one of which is shown as an example in Fig. 2.

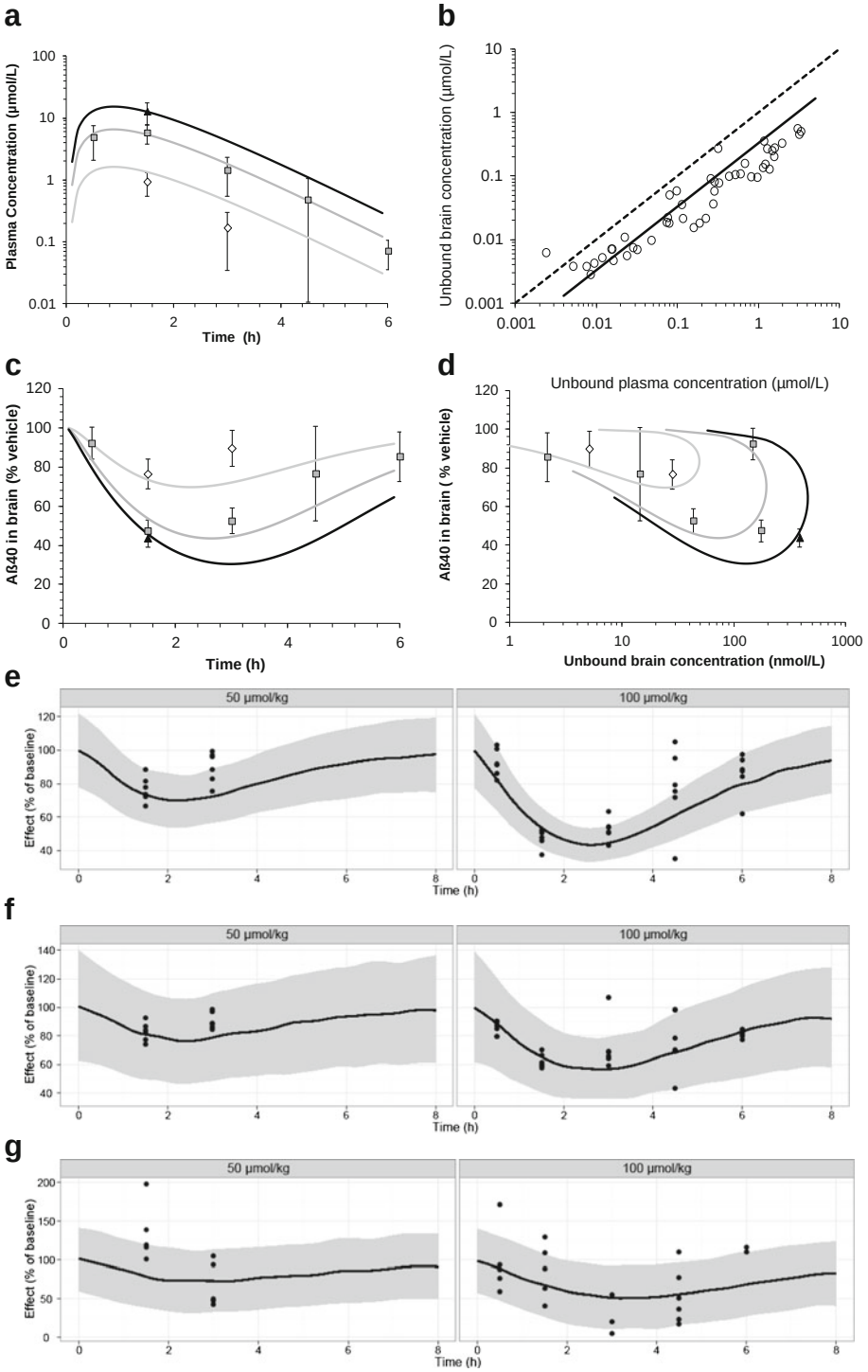

Fig. 2 Compound 1 dosed at 50 (diamonds), 100 (squares) or 200 (triangles) μmol/kg p.o. to male Dunkin-Hartley guinea pigs at $t = 0$. (**a**) Mean ± SD observed and fitted by naïve pooled analysis in WinNonlin plasma exposure. (**b**) Unbound plasma *versus* brain exposure. (**c**) Mean ± SD observed and population fitted Aβ40 (% change from vehicle) in brain after oral dosing. (**d**) Observed and population fitted unbound brain concentrations *versus* Aβ40 inhibition in brain. (**e**) Individual time *versus* Aβ40 in brain observations and the 95% prediction interval after a 50 and 100 μmol/kg dose. (**f**) Individual time *versus* Aβ42 in brain observations and the 95% prediction interval after a 50 and 100 μmol/kg dose. (**g**) Individual time *versus* Aβ40 in CSF observations and the 95% prediction interval after a 50 and 100 μmol/kg dose.

Compound 1 was orally administered at doses 50, 100 and 200 µmol/kg. Exposure in plasma was fitted simultaneously for these doses. A dose-dependent absorption was allowed to account for the dose-dependent exposure. A 4-fold increase in exposure was observed between doses 50 and 100 µmol/kg while doubling the dose. A one-compartment PK model fitted the data best, with an apparent clearance 6.8 L/h/kg (CV 14%), apparent volume 4.7 L/kg (CV 61%) and absorption rate constant of 1.0 h^{-1} (CV 35%). The plasma exposure reached C_{max} at around 1 h after the dose (Fig. 2a). The

Table III Population System Parameter Estimates in Mouse and Guinea Pig with the Relative Error of the Mean (%)

	I_{max} (%)	k_{out} (h^{-1})	$T_{1/2}$ k_{out} (min)
Mouse			
Aβ40 in brain vs unbound brain exposure	85 (3%)	1.5 (7%)	28
Guinea pig			
Aβ40 in brain vs unbound brain exposure	100[a]	0.7 (4%)	60
Aβ42 in brain vs unbound brain exposure	83 (15%)	0.6 (23%)	69
Aβ40 in brain vs unbound plasma exposure	100 (7%)	0.6 (9%)	65
Aβ40 in CSF vs unbound plasma exposure	100 (16%)	0.4 (22%)	115

[a] Value indirectly estimated using Eq. 3

relationship between unbound plasma and brain concentration was linear with a ratio of 0.33 for all time points and doses (Fig. 2b).

Population parameter estimates for *in vivo* potency are listed in Table II, and the population estimates for the system-specific parameters are listed in Table III. The inclusion of a slope factor *n* did not improve the estimates and was therefore fixed to 1. In Fig. 2c and d the mean ± SD observations are shown with the population fit. A clear hysteresis loop was observed. The turnover half-life was estimated around 1 h for brain Aβ40 and brain Aβ42. This was independent of using plasma or brain concentration in the analysis. The turnover half-life of Aβ40 in CSF was almost 2 h (Table III). The 95% prediction intervals were explored by simulation of 1,000 runs and the variability of the population estimates and are shown together with the individual observations for the 50 and 100 μmol/kg doses for brain Aβ40, brain Aβ42 and CSF Aβ40 in Fig. 2e, f and g, respectively. The goodness-of-fit of the population analysis of brain exposure *versus* brain Aβ40 was evaluated in Fig. 3c ($R = 0.70$, $P < 0.01$) and d. The conditional weighted residuals (CWRES) *versus* time were concentrated around the 0 line (Fig. 3d) similarly to the mouse data analysis.

In Vitro Correlations

Guinea pig primary cortical neurons (PCN) were successfully isolated and cultured as shown in Fig. 4a. In mice a PCN isolation and culture method was already available which allowed evaluation of the suitability of the mouse N2A cell line for screening purposes. Compounds with a wide range of potency were tested in our *in vitro* systems. In mouse and guinea pig PCN and in the N2A mouse cell line our BACE1 inhibitors displayed a concentration dependent inhibition of Aβ release, exemplified with compound 5 in mouse PCN

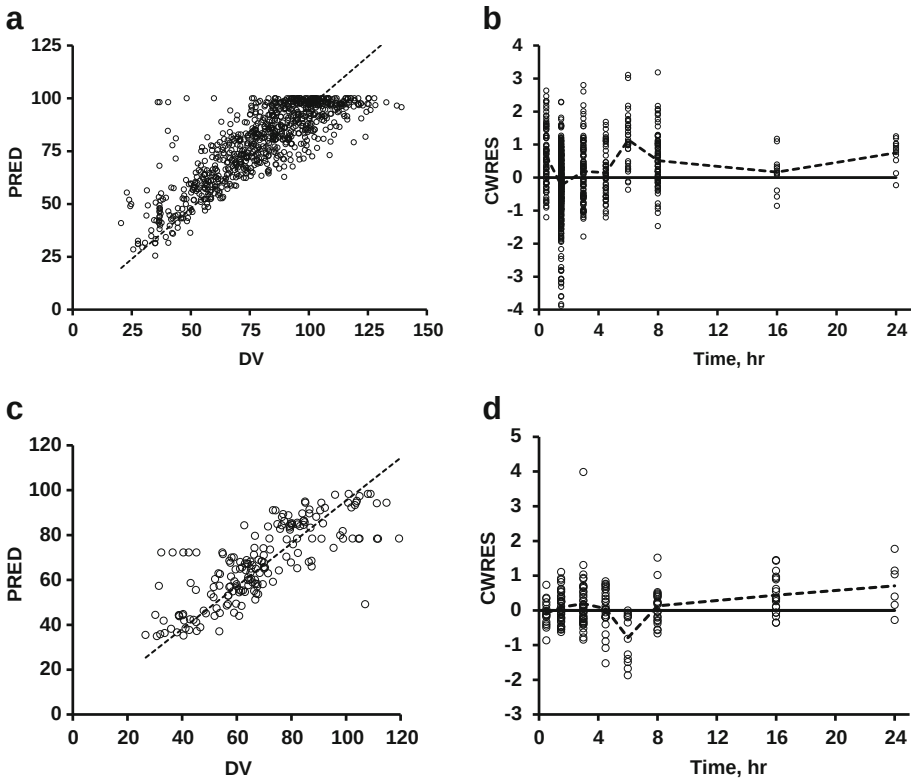

Fig. 3 Goodness of fit. (**a**) Predicted (PRED) *versus* observed (DV) Aβ40 levels in brain in individual mice. (**b**) Individual and mean (*dashed line*) conditional weighted residuals (CWRES) of Aβ40 in brain *versus* time of mice. (**c**) Predicted (PRED) *versus* observed (DV) Aβ40 levels in brain in individual guinea pigs. (**d**) Individual and mean (*dashed line*) conditional weighted residuals (CWRES) of Aβ40 in brain *versus* time of guinea pigs.

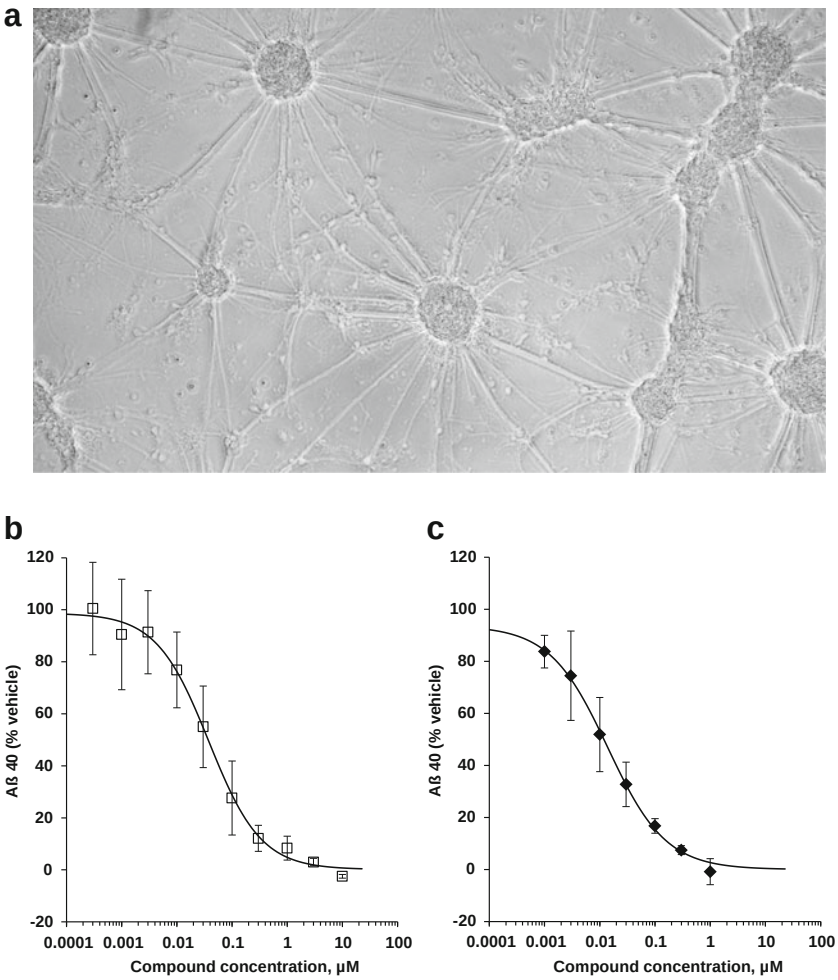

Fig. 4 *In vitro* inhibition of Aβ40 secretion by primary cortical neurons. (**a**) Visualization of guinea pig primary cortical neurons in culture. (**b**) Normalized secreted Aβ40 levels *versus* concentration of compound 5 in medium of mouse primary cortical neurons. (**c**) Normalized secreted Aβ40 levels *versus* concentration of compound 1 in medium of guinea pig primary cortical neurons.

(Fig. 4b) and compound 1 in guinea pig PCN (Fig. 4c). A near 1:1 correlation was observed for the IC_{50}s determined in the N2A cell line and in mouse PCN (Fig. 5a) for 25 compounds, demonstrating no shift between a cell-line and a primary culture of the same species. Potency in human SH-SY5Y cells was strongly correlated to potency in mouse (n=73) and guinea pig (n=25) PCN with a similar 4.5-fold lower IC_{50} value observed in the SH-SY5Y cells (Fig. 5b). For compounds dosed *in vivo* the *in vitro* IC_{50} values are presented in Tables I and II.

In Vitro-In Vivo Correlations

IC_{50} values from *in vitro* PCN and estimated IC_{50}s from the population analysis *in vivo* were compared. There was a clear correlation between the IC_{50} to inhibit Aβ40 release in PCN cells *in vitro* and the IC_{50} estimated free brain concentration *in vivo* both for mouse and guinea pig (Fig. 6). The mouse time response data had a correlation coefficient R of 0.85 (n=10, $P<0.01$) and the dose response of 0.72 (n=22, $P<0.01$), indicating a clear linear relationship. Due to the limited number of guinea pig data points, no statistical analysis was reported.

DISCUSSION

In the present paper, a population modeling approach was used to quantify the compound-specific *in vivo* potencies of BACE1 inhibitors, as well as the system-specific Aβ turnover rate. The turnover half-life of Aβ40 in brain was 0.5 h in mouse and 1 h in guinea pig. For CSF, the turnover half-life of Aβ40 was 2 h. A good correlation was observed between *in vitro* potency in primary cortical neurons (PCN) and *in vivo* unbound brain potency. For the mouse *in vitro* assays, a clear correlation was found between potency in N2A cells and PCN. In addition, a constant 4.5-fold higher potency was found, when comparing, over a wide concentration range, the potency in a human cell line to the potency in PCN.

The amyloid hypothesis is central for BACE1 involvement in AD. New chemical entities are often tested in wild-type mice and/or transgenic mouse models that over-express human APP (31). Asai *et al.* (50) performed intra-hippocampal

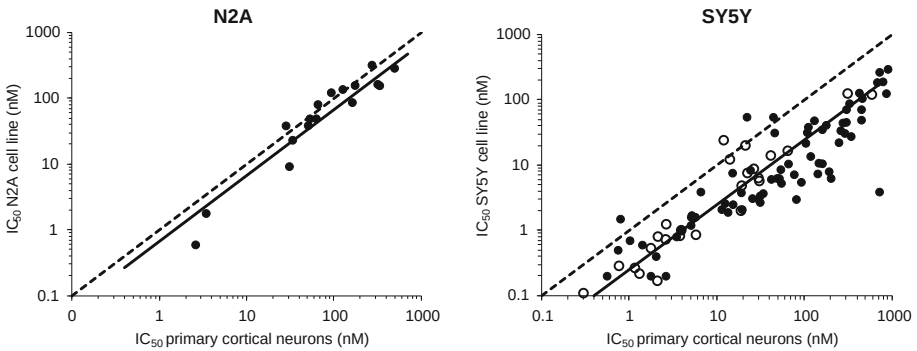

Fig. 5 *Left*: *In vitro* potency in the mouse primary cortical neurons *versus* potency in the mouse N2A cell line ($n = 17$). *Right*: Potency in the human SH-SY5Y cell line *versus* potency *in vitro* in the mouse (*solid circles*, n = 73) and guinea pig (*open circles*, n = 25) primary cortical neurons. Regression line for correlation was similar for mouse and guinea pig.

injection as a proof of concept of BACE1 inhibition in wild type mice. Two doses of the drug reduced the Aβ levels in brain. Unfortunately, no time-response or exposure information was reported. Nishitomi *et al.* (27) demonstrated BACE1 inhibition in wild type mice with significant reduction of Aβ40 levels in brain, but without reporting exposure levels or a time-response profile. Our work demonstrated that modeling of concentration-effect data, while taking the Aβ turnover rate and the unbound brain fraction into account, allowed for the estimation of the potency in the brain. Our findings are in agreement with two previous BACE1 inhibition time-response studies that reported a turnover-rate of brain Aβ in wild type mice of 0.5 h (28,29). In clinical development, Aβ reduction in CSF is the central read-out to monitor BACE1 target engagement. Niva *et al.* (16) demonstrated that Aβ effects in animal brain were relatively good predictors of human Aβ response in CSF (and putatively in brain). CSF sampling has been reported in mice, making mice an adequate *in vivo* model to study CSF and brain effect (51). Lowering of CSF and brain Aβ by BACE1 inhibition has been reported in guinea pig after repeated doses (52), and, more recently, also in time-response studies after a single dose (28,29,40). In a study with AZD3839, the turnover half-life of Aβ40 was estimated to be around 1 h in brain and 44 min in CSF, which is slightly faster than the population estimates reported in this paper (29). However, in this paper, the results of many combined experiments may have increased the accuracy of the turnover estimate. The turnover rate of Aβ is a system-specific parameter, and therefore should be constant within a species and within a compartment (CSF, brain, plasma). Understanding the turnover rate of Aβ in each species and each compartment allows for interspecies translation. When the system-specific parameters have been established, there is no need to re-assess them in each future *in vivo* experiment. Analysis of dose–response experiments can be sufficient to estimate potency, as long as the prior estimated system parameters are taken into account. Interestingly, in a recent investigation, an interspecies relationship between body weight and turnover rate for Aβ in the CSF was demonstrated (53). This allometric relationship is in accordance to the compound- and system-specific concepts in mechanism-based modeling approaches (54,55). *In vitro* cultured PCN have been widely used to determine potency of BACE1 inhibition in a number of species such as mouse (27), rat (56), and guinea pig (16,29). It was shown that *in vitro* guinea pig primary brain cells produced APP, and that Aβ was secreted into the medium (57). To our knowledge, the work described in this paper demonstrates for the first time that cultured guinea pig PCN were used to screen BACE1 inhibitors in a reproducible manner over a wide range of potencies. The mouse and guinea pig PCN assays were used to explore species differences in potency. Moreover, the potency observed in PCN cells correlated well to the potency observed in the human SH-SY5Y cell line; a systematic lower potency was observed in PCN (4.5-fold for mice and 4-fold for guinea pig) over a wide potency range. This ratio might be due to species differences in enzymatic efficiency as reported for

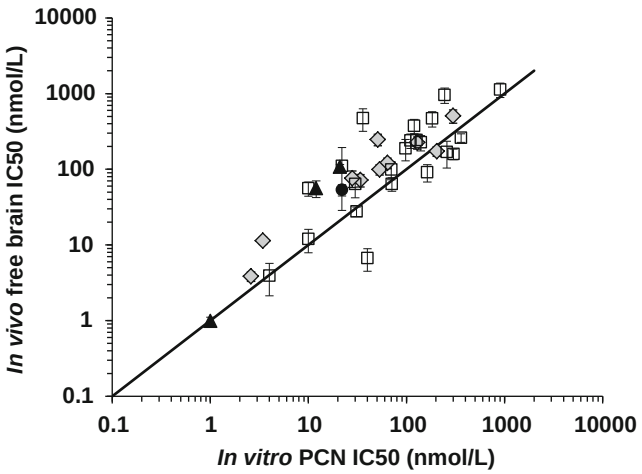

Fig. 6 *In vitro-in vivo* correlations. IC_{50} estimated in a population analysis using the indirect response model based on free brain concentrations *versus* IC_{50} in primary mouse or guinea pig neurons *in vitro*, respectively. *Diamonds* represent estimates from mouse time-response experiments; *squares* represent estimates from mouse dose–response experiments; *triangles* represent estimates from guinea pig time-response experiments; and *circles* represent estimates from guinea pig dose–response experiments.

mouse and human (58). Therefore, such correlations should be established in each laboratory and for each assay.

To our knowledge, there is no suitable guinea pig cell line that allows testing of BACE1 inhibition. For mouse, however, the potency in N2A cell line showed a 1:1 relationship to the mouse PCN potency. Therefore, these primary neuronal cells could be replaced by the N2A cell line, allowing reduction of laboratory animal use following the 3R principle (refine, reduce, replace). The N2A cell line could also be used to test γ-secretase inhibition or modulation (59), although its translation would need to be confirmed (16).

When translating *in vitro* data to *in vivo*, not only the exposure and effect have to be considered, but also the unbound brain-plasma ratio and the turnover rate of Aβ in the respective compartments. As shown in this paper, compounds 1 and 5 did not show any delay in establishment of equilibrium of compound concentrations between brain and plasma. A delay in onset of Aβ effect, however, was expected, since BACE1 inhibition can only be observed after turnover of existing Aβ, and, hence, required time-resolved data. Ignoring this delay could lead to false estimates of compound potency. All observations per compound were pooled for estimation of the IC_{50}, while the turnover delay and I_{max} were estimated as population parameters for all compounds simultaneously. This approach did not explore the pharmacokinetic profile of each compound nor the possibility of non-linear kinetics. The observed unbound brain concentrations were used to avoid making any assumptions on the pharmacokinetic profile and distribution to the brain. For 32 compounds in mice and 4 compounds in guinea pig, unbound brain IC_{50}s were estimated, as well as single Aβ turnover rates for Aβ in the various compartments. The unbound potencies showed an 1:1 correlation to the *in vitro* IC_{50}s, indicating that potency *in vitro* directly translates to *in vivo*. In contrast, Wood *et al.*, (37) did not detect a good predictive value of an *in vitro* assay when screening 134 compounds in rat. A potential explanation could be that in this investigation the total plasma concentrations were used without correcting for the unbound plasma-to-brain distribution. These compound properties can differ substantially and, thereby, mask a potential correlation. In addition, if the time-delay in the response is ignored, an over- or under- estimation of potency can occur, depending on when the samples are taken (60).

How can we improve our *in vivo* study design and screening cascade? First, population pharmacokinetic-pharmacodynamic approach should be applied, analyzing all data simultaneously. This allows accurate estimation of potency for compounds, tested in a dose–response design, by using the information on turnover rate of Aβ from time-course experiments. Second, when a good *in vitro-in vivo* correlation of potency is established, there is a reduced need for running *in vivo* experiments. Only promising compounds, based on *in vitro* assay, should be confirmed *in vivo*. The exposure-effect relationship can be achieved with fewer animals, since not all dose levels need to be studied in a time-course design. Should the project move away from the specific chemical space in which these correlations were established, confirmation of the *in vitro-in vivo* relationship would be needed. It is, however, important to continuously assess the compound's pharmacokinetic properties, brain penetration, and binding. However, replacement of any of these assays by an *in vitro* equivalent, and the improved design of *in vivo* experiments will increase the quality of studies performed and reduce the number of animals.

CONCLUSION

A good correlation between *in vitro* and *in vivo* potency for mouse and guinea pig, and an excellent correlation between potency in PCN and human SH-SY5Y cells, increased the confidence in using human cell lines for screening and optimization for effects of novel BACE1 inhibitors. Moreover, the established *in vitro-in vivo* correlations can optimize the design and reduce the number of preclinical *in vivo* effect studies.

ACKNOWLEDGMENTS AND DISCLOSURES

The authors would like to thank Eva Spennare for determining the fraction unbound in brain; Jenny Johansson for measuring the plasma protein binding; Hongmei Yan for collecting the data into the data-analysis sheet; Sveinn Briem and his team for performing the bioanalysis; Elin Lundkvist and Fredrik Olsson for supporting the *in vitro* experiments; and Kristina Eliason for supporting the *in vivo* experiments.

REFERENCES

1. McKhann G, Drachman D, Folstein M, Katzman R, Price D, Stadlan EM. Clinical diagnosis of Alzheimer's disease: report of the NINCDS-ADRDA Work Group under the auspices of Department of Health and Human Services Task Force on Alzheimer's Disease. Neurology. 1984;34(7):939–44.
2. Querfurth HW, LaFerla FM. Alzheimer's disease. N Engl J Med. 2010;362(4):329–44.
3. Alzheimer's Association. Alzheimer's disease facts and figures. Alzheimers Dement. 2012;8(2):131–68.
4. Hardy J. The amyloid hypothesis for Alzheimer's disease: a critical reappraisal. J Neurochem. 2009;110(4):1129–34.
5. Karran E, Mercken M, De Strooper B. The amyloid cascade hypothesis for Alzheimer's disease: an appraisal for the development of therapeutics. Nat Rev Drug Discov. 2011;10(9):698–712.
6. Wolfe MS. gamma-Secretase inhibitors and modulators for Alzheimer's disease. J Neurochem. 2012;120 Suppl 1:89–98.
7. Walsh DM, Teplow DB. Alzheimer's disease and the amyloid β-protein. Prog Mol Biol Transl Sci. 2012;107:101–24.

8. Lichtenthaler SF, Haass C, Steiner H. Regulated intramembrane proteolysis–lessons from amyloid precursor protein processing. J Neurochem. 2011;117(5):779–96.
9. Hardy J, Selkoe DJ. The amyloid hypothesis of Alzheimer's disease: progress and problems on the road to therapeutics. Science. 2002;297(5580):353–6.
10. Iwatsubo T, Odaka A, Suzuki N, Mizusawa H, Nukina N, Ihara Y. Visualization of Aβ 42(43) and Aβ 40 in senile plaques with end-specific Aβ monoclonals: evidence that an initially deposited species is Aβ 42(43). Neuron. 1994;13(1):45–53.
11. Younkin SG. Evidence that Aβ 42 is the real culprit in Alzheimer's disease. Ann Neurol. 1995;37(3):287–8.
12. Steiner H, Capell A, Leimer U, Haass C. Genes and mechanisms involved in β-amyloid generation and Alzheimer's disease. Eur Arch Psychiatr Clin Neurosci. 1999;249(6):266–70.
13. Citron M. Alzheimer's disease: strategies for disease modification. Nat Rev Drug Discov. 2010;9(5):387–98.
14. Panza F, Frisardi V, Imbimbo BP, Capurso C, Logroscino G, Sancarlo D, *et al*. REVIEW: gamma-Secretase inhibitors for the treatment of Alzheimer's disease: the current state. CNS Neurosci Ther. 2010;16(5):272–84.
15. Kreft AF, Martone R, Porte A. Recent advances in the identification of gamma-secretase inhibitors to clinically test the Aβ oligomer hypothesis of Alzheimer's disease. J Med Chem. 2009;52(20):6169–88.
16. Niva C, Parkinson J, Olsson F, van Schaick EA, Lundkvist J, Visser SAG. Has inhibition of Aβ production adequately been tested as therapeutic approach in mild AD? A model-based meta-analysis of γ-secretase inhibitor data. Eur J Clin Pharmacol. 2013. doi:10.1007/s00228-012-1459-3.
17. Hussain I, Powell D, Howlett DR, Tew DG, Meek TD, Chapman C, *et al*. Identification of a novel aspartic protease (Asp 2) as β-secretase. Mol Cell Neurosci. 1999;14(6):419–27.
18. Sinha S, Anderson JP, Barbour R, Basi GS, Caccavello R, Davis D, *et al*. Purification and cloning of amyloid precursor protein β-secretase from human brain. Nature. 1999;402(6761):537–40.
19. Vassar R, Bennett BD, Babu-Khan S, Kahn S, Mendiaz EA, Denis P, *et al*. β-secretase cleavage of Alzheimer's amyloid precursor protein by the transmembrane aspartic protease BACE. Science. 1999;286(5440):735–41.
20. Yan R, Bienkowski MJ, Shuck ME, Miao H, Tory MC, Pauley AM, *et al*. Membrane-anchored aspartyl protease with Alzheimer's disease β-secretase activity. Nature. 1999;402(6761):533–7.
21. Lin X, Koelsch G, Wu S, Downs D, Dashti A, Tang J. Human aspartic protease memapsin 2 cleaves the β-secretase site of β-amyloid precursor protein. Proc Natl Acad Sci U S A. 2000;97(4):1456–60.
22. Cole SL, Vassar R. BACE1 structure and function in health and Alzheimer's disease. Curr Alzheimer Res. 2008;5(2):100–20.
23. Stockley JH, O'Neill C. The proteins BACE1 and BACE2 and β-secretase activity in normal and Alzheimer's disease brain. Biochem Soc Trans. 2007;35(Pt 3):574–6.
24. Mullan M, Houlden H, Windelspecht M, Fidani L, Lombardi C, Diaz P, *et al*. Nat Genet. 1992;2(4):340–2.
25. Jonsson T, Atwal JK, Steinberg S, Snaedal J, Jonsson PV, Bjornsson S, *et al*. A mutation in APP protects against Alzheimer's disease and age-related cognitive decline. Nature. 2012;488(7409):96–9.
26. McConlogue L, Buttini M, Anderson JP, Brigham EF, Chen KS, Freedman SB, *et al*. Partial reduction of BACE1 has dramatic effects on Alzheimer plaque and synaptic pathology in APP Transgenic Mice. J Biol Chem. 2007;282(36):26326–34.
27. Nishitomi K, Sakaguchi G, Horikoshi Y, Gray AJ, Maeda M, Hirata-Fukae C, *et al*. BACE1 inhibition reduces endogenous Aβ and alters APP processing in wild-type mice. J Neurochem. 2006;99(6):1555–63.
28. Swahn BM, Kolmodin K, Karlstrom S, von Berg S, Soderman P, Holenz J, *et al*. Design and synthesis of β-Site Amyloid Precursor Protein Cleaving Enzyme (BACE1) inhibitors with in vivo brain reduction of β-Amyloid peptides. J Med Chem. 2012;55(21):9346–61.
29. Jeppsson F, Eketjall S, Janson J, Karlstrom S, Gustavsson S, Olsson LL, *et al*. Discovery of AZD3839, a potent and selective BACE1 clinical candidate for the treatment of Alzheimers Disease. J Biol Chem. 2012;287(49):41245–57.
30. Lu Y, Zhang L, Nolan CE, Becker SL, Atchison K, Robshaw AE, *et al*. Quantitative pharmacokinetic/pharmacodynamic analyses suggest that the 129/SVE mouse is a suitable preclinical pharmacology model for identifying small-molecule gamma-secretase inhibitors. J Pharmacol Exp Ther. 2011;339(3):922–34.
31. Stachel SJ, Coburn CA, Sankaranarayanan S, Price EA, Wu G, Crouthamel M, *et al*. Macrocyclic inhibitors of β-secretase: functional activity in an animal model. J Med Chem. 2006;49(21):6147–50.
32. Stanton MG, Stauffer SR, Gregro AR, Steinbeiser M, Nantermet P, Sankaranarayanan S, *et al*. Discovery of isonicotinamide derived β-secretase inhibitors: in vivo reduction of β-amyloid. J Med Chem. 2007;50(15):3431–3.
33. Fukumoto H, Takahashi H, Tarui N, Matsui J, Tomita T, Hirode M, *et al*. A noncompetitive BACE1 inhibitor TAK-070 ameliorates Aβ pathology and behavioral deficits in a mouse model of Alzheimer's disease. J Neurosci. 2010;30(33):11157–66.
34. Chang WP, Huang X, Downs D, Cirrito JR, Koelsch G, Holtzman DM, *et al*. β-secretase inhibitor GRL-8234 rescues age-related cognitive decline in APP transgenic mice. FASEB J. 2011;25(2):775–84.
35. Lu Y, Riddell D, Hajos-Korcsok E, Bales K, Wood KM, Nolan CE, et al. CSF Aβ As An Effect Biomarker For Brain Aβ Lowering Verified by Quantitative Preclinical Analyses. J Pharmacol Exp Ther. 2012;342(2):366–75.
36. Rueeger H, Lueoend R, Rogel O, Rondeau JM, Mobitz H, Machauer R, *et al*. Discovery of cyclic sulfone hydroxyethylamines as potent and selective β-site APP-cleaving enzyme 1 (BACE1) inhibitors: structure-based design and in vivo reduction of amyloid β-peptides. J Med Chem. 2012;55(7):3364–86.
37. Wood S, Wen PH, Zhang J, Zhu L, Luo Y, Babu-Khan S, *et al*. Establishing the relationship between in vitro potency, pharmacokinetic, and pharmacodynamic parameters in a series of orally available, hydroxyethylamine-derived β-secretase inhibitors. J Pharmacol Exp Ther. 2012;343(2):460–7.
38. Weiss MM, Williamson T, Babu-Khan S, Bartberger MD, Brown J, Chen K, *et al*. Design and preparation of a potent series of hydroxyethylamine containing β-secretase inhibitors that demonstrate robust reduction of central β-amyloid. J Med Chem. 2012;55(21):9009–24.
39. Dineen TA, Weiss MM, Williamson T, Acton P, Babu-Khan S, Bartberger MD, *et al*. Design and synthesis of potent, orally efficacious hydroxyethylamine derived β-site amyloid precursor protein cleaving enzyme (BACE1) inhibitors. J Med Chem. 2012;55(21):9025–44.
40. Gravenfors Y, Viklund J, Blid J, Ginman T, Karlstrom S, Kihlstrom J, *et al*. New Aminoimidazoles as β-Secretase (BACE-1) inhibitors showing amyloid-β (Aβ) lowering in Brain. J Med Chem. 2012;55(21):9297–311.
41. Sankaranarayanan S, Holahan MA, Colussi D, Crouthamel MC, Devanarayan V, Ellis J, *et al*. First demonstration of cerebrospinal fluid and plasma Aβ lowering with oral administration of a β-site amyloid precursor protein-cleaving enzyme 1 inhibitor in nonhuman primates. J Pharmacol Exp Ther. 2009;328(1):131–40.
42. May PC, Dean RA, Lowe SL, Martenyi F, Sheehan SM, Boggs LN, *et al*. Robust central reduction of amyloid-β in humans with an orally available, non-peptidic β-secretase inhibitor. J Neurosci. 2011;31(46):16507–16.
43. Swahn BM, Holenz J, Kihlstrom J, Kolmodin K, Lindstrom J, Plobeck N, *et al*. Aminoimidazoles as BACE-1 inhibitors: the challenge to achieve in vivo brain efficacy. Bioorg Med Chem Lett. 2012;22(5):1854–9.

44. Bueters T, Dahlstrom J, Kvalvagnaes K, Betner I, Briem S. High-throughput analysis of standardized pharmacokinetic studies in the rat using sample pooling and UPLC-MS/MS. J Pharm Biomed Anal. 2011;55(5):1120–6.
45. Heisey SR. Brain and choroid plexus blood volumes in vertebrates. Comp Biochem Physiol. 1968;26(2):489–98.
46. Park S, Sinko PJ. P-glycoprotein and mutlidrug resistance-associated proteins limit the brain uptake of saquinavir in mice. J Pharmacol Exp Ther. 2005;312(3):1249–56.
47. Borgegård T, Minidis A, Jureus A, Malmborg J, Rosqvist S, Gruber, S., Almqvist, H., et al. In vivo analysis using a presenilin-1-specific inhibitor: Presenilin 1- containing g-secretase complexes mediate the majority of CNS Ab production in the mouse. 3 2011;1:30–45.
48. Friden M, Ducrozet F, Middleton B, Antonsson M, Bredberg U, Hammarlund-Udenaes M. Development of a high-throughput brain slice method for studying drug distribution in the central nervous system. Drug Metab Dispos. 2009;37(6):1226–33.
49. Dayneka NL, Garg V, Jusko WJ. Comparison of four basic models of indirect pharmacodynamic responses. J Pharmacokinet Biopharm. 1993;21(4):457–78.
50. Asai M, Hattori C, Iwata N, Saido TC, Sasagawa N, Szabo B, *et al*. The novel β-secretase inhibitor KMI-429 reduces amyloid β peptide production in amyloid precursor protein transgenic and wild-type mice. J Neurochem. 2006;96(2):533–40.
51. Liu L, Duff K. A technique for serial collection of cerebrospinal fluid from the cisterna magna in mouse. J Vis Exp 2008 Nov 10;(21).
52. Truong AP, Toth G, Probst GD, Sealy JM, Bowers S, Wone DW, *et al*. Design of an orally efficacious hydroxyethylamine (HEA) BACE-1 inhibitor in a preclinical animal model. Bioorg Med Chem Lett. 2010;20(21):6231–6.
53. Lu Y. Integrating experimentation and quantitative modeling to enhance discovery of Beta amyloid lowering therapeutics for Alzheimer's disease. Front Pharmacol. 2012;3(177):1–6.
54. Danhof M, Van der Graaf PH, Jonker DM, Visser SAG, Zuideveld KP. Mechanism-based pharmacokinetic-pharmacodynamic modeling for the prediction of in vivo drug concentration-effect relationships -application in drug candidate selection and lead optimization. 2007. Comprehensive Medicinal Chemistry (2nd Ed.) Volume 5: "ADME-Tox: The Fate of Drugs in the Body". Editors Bernard Testa and Han van de Waterbeemd.
55. Bueters T, Ploeger BA, Visser SA. The virtue of translational PKPD modeling in drug discovery: selecting the right clinical candidate while sparing animal lives. Drug Discov Today. 2013. doi:10.1016/j.drudis.2013.05.001.
56. Shimmyo Y, Kihara T, Akaike A, Niidome T, Sugimoto H. Flavonols and flavones as BACE-1 inhibitors: structure-activity relationship in cell-free, cell-based and in silico studies reveal novel pharmacophore features. Biochim Biophys Acta. 2008;1780(5):819–25.
57. Beck M, Bruckner MK, Holzer M, Kaap S, Pannicke T, Arendt T, *et al*. Guinea-pig primary cell cultures provide a model to study expression and amyloidogenic processing of endogenous amyloid precursor protein. Neuroscience. 2000;95(1):243–54.
58. Yang HC, Chai X, Mosior M, Kohn W, Boggs LN, Erickson JA, *et al*. Biochemical and kinetic characterization of BACE1: investigation into the putative species-specificity for β- and β'-cleavage sites by human and murine BACE1. J Neurochem. 2004;91(6):1249–59.
59. Vandermeeren M, Geraerts M, Pype S, Dillen L, Van Hove C, Mercken M. The functional gamma-secretase inhibitor prevents production of amyloid β 1–34 in human and murine cell lines. Neurosci Lett. 2001;315(3):145–8.
60. Gabrielsson J, Fjellstrom O, Ulander J, Rowley M, Van Der Graaf PH. Pharmacodynamic-pharmacokinetic integration as a guide to medicinal chemistry. Curr Top Med Chem. 2011;11(4):404–18.